

Effect of Selenium Doping on Corrosion and Electrochemical Performance of Pb-Sb-As-Se Alloys as Positive Grids in Hybrid Lead-Acid Batteries

Z. Ghasemi, A. Tizpar*

R&D of Niru Battery Manufacturing CO., Pasdaran, P.O. Box 19575-361, Tehran, Iran

*E-mail: atizpar@yahoo.com

Received: 1 January 2008 / *Accepted:* 22 March 2008 / *Online published:* 20 April 2008

The effect of selenium as an alloying additive on the electrochemical behavior, corrosion resistance and microstructure of Pb-Sb-As alloys as positive grids of hybrid lead-acid batteries was studied. This investigation was performed by means of weight-loss measurements, Potentiodynamic Sweeping (PS), cyclic voltammetry, electrochemical impedance spectroscopy (EIS), hardness measurements and optical microscopy. Studies on Pb-Sb-As-Se alloys (Se=0.007, 0.0108, 0.0141 and 0.0207 wt%) indicate that with increasing selenium concentration in the alloy composition, corrosion currents and corrosion rates decrease and corrosion potentials shift to negative values and the variations are proportional to selenium contents. In addition, selenium increases hydrogen and oxygen evolution reaction overpotentials. So, it decreases the rate of gas evolution reaction in lead acid batteries. The electrochemical impedance of oxide film on the alloy with selenium is much larger than that of the oxide formed on the Pb-Sb-As alloy and it increases with increasing selenium content in the alloy. The a.c. impedance data show that the high content of selenium greatly inhibits the growth of passivation layer and increases the polarization resistance of the alloys. Optical microscopy was used to study the microstructure of Pb-Sb-As alloys with different concentrations of selenium. The results show that, selenium has an important role in reducing the size of the grains and causes to decrease the reduction reaction of PbO₂ to PbSO₄ that means corrosion resistance of the alloy increases. Also, selenium addition increases the hardness of Pb-Sb-As alloy that it is more considerable in the high selenium contents. The discharge capacities of lead-acid batteries made of these grids by using Pb-Ca grids as negative electrodes were investigated. The results during the first 25 cycles show that selenium has a beneficial effect on discharge capacities during the later cycles.

Keywords: lead-acid battery; selenium; corrosion; grain boundary; gas evolution

1. INTRODUCTION

The most critical non-active component in a lead-acid battery is the grid. This is used to support the positive and negative active materials, and also to provide a conductive path for the current

to and from the plates during charge and discharge. Lead as a malleable metal, is generally too soft to be used as a production grid material, except for a few battery types that utilize pure lead for high performance and life. As a result of many investigations by battery workers by the end of the first half of the twentieth century, various lead alloys had become established. Numerous lead alloys have been tested for the manufacture of grids of pasted batteries especially Pb-Ca and Pb-Sb without or with other elements. Although many lead alloys have desirable mechanical and casting properties, they suffer more or less from electrochemical corrosion, mostly due to overcharging and self-discharging. The main alloying system used in grids was lead-antimony. This was usually based on the eutectic composition of about 11wt% antimony as such an alloy was easy to cast into the complex form required for battery grids [1-2]. Antimony is used to strengthen and harden the lead grids for improved handling and casting, as well as having good conductive properties. At one time almost all lead-acid batteries were made with lead-antimony grids, and the original antimony alloy concentrations were in 8-12% range (Today the more common concentration levels we see in batteries using lead-antimony alloys are in the 4-6% range) [3]. Antimony additive has some advantages and some disadvantages. On the one hand antimony stabilizes the active material of the positive electrode, the cycle life of the battery is improved and passivation effects disturbing mainly the discharge are not observed when alloys with high antimony content are used for positive grids. On the other hand, antimony migrates to the negative plate where it is precipitated there and reduces the hydrogen over voltage. This leads to lower charge voltage, increased self-discharge and therefore increased water loss of the battery. In addition to the mechanical strength required for further treatment of the grids, the castability is another important factor for producing sound grids at tolerable costs. The main difficulty with casting low antimony alloys is that the decrease of antimony content is accompanied by the appearance of hot cracks, if no special precautions are taken [2]. The development of low-maintenance and maintenance-free batteries and the move towards purer systems, with no poisoning of the negative plate, has resulted in the use of binary lead calcium grids in the negative plates of hybrid batteries [1]. For improving the castability of low-antimony alloys, some alloying additives are used. One of these main additives is selenium. Selenium is a grain refiner which, when used in combination with other elements, such as arsenic also help to increase the alloy rigidity and correspondingly eases plant handling of the materials [4-7]. This addition forms a fine globulitic solidification which results in fewer casting faults and it refines grain size. The formation of dendrites, which disturbs the feeding capacity of the mould during casting and leads to casting faults, is almost fully suppressed. With fine globulitic solidification, uniform mechanical properties are achieved in all directions, and hence the ductility is increased [8-14]. Selenium is toxic. Lead producers have equipment and procedures to allow safe handling, and it is quite safe when incorporated in a battery alloy. In use, it can be lost to the dross on excessive cooling or on freezing and remelting. Occasionally, requests have been received for selenium master alloys, or for advice on adding selenium to a melt which has become deficient. It is recommended that anyone without the required equipment or expertise should not add selenium [15].

The effect of selenium on Pb and Pb-Sn alloy was investigated by some authors, but there is not a complete research about the influence of selenium on electrochemical behavior, corrosion resistance and microstructure of Pb-Sb-As alloys. Pb-Sb-As-Se alloys are used as positive grids of hybrid lead- acid batteries at Niru Battery Manufacturing Company in Iran. The aim of this work is

investigation of the effect of selenium addition to Pb-Sb-As alloy on battery characteristics, gas evolution behavior, positive grid corrosion and hardness of grid alloy. Also we study selenium effect as a grain refiner on battery grids using optical microscopy.

2. EXPERIMENTAL PART

2.1. PS, CV, EIS

A nominal alloy composition (Pb-1.8wt%Sb- 0.1wt%As) was used as the base alloy. Selenium was added to the molten alloy in the range of 0.007-0.0207wt% at about 700°C. The alloys with different concentrations of selenium were shaped into rods and sealed with epoxy resin leaving a working surface of 0.08cm² exposed for each electrode. Before being subjected to the sulfuric acid medium, the surface of working electrodes were polished mechanically with emery papers 800, 1500, 2500 and thoroughly rinsed with double-distilled water. A platinum plate served as a counter electrode and an Hg/Hg₂SO₄ electrode was used as the reference electrode. All potentials are referred to this scale. Potentiodynamic sweeping was carried out using a galvanostate/potentiostate Autolab (PCSTA T20) apparatus connected to a PC computer. Before every experiment a cathodic polarization at -1.6V for 10 min was performed to remove any oxidation products formed during pretreatment. Polarization curves were recorded in the potential range of -1.2 to -0.95V. The electrolyte was 1.28 sp.gr. H₂SO₄ solution.

Cyclic voltammetry measurements were performed to investigate the anodic layer formation and gas evolution reactions. Cyclic voltammograms were recorded at a scan rate of 20 mVs⁻¹ in the PbO₂/PbSO₄ couple potential region (0.9-1.6 V vs Hg/Hg₂SO₄) for 50 cycles and oxygen and hydrogen evolution potential regions. EIS measurements were performed with an electrochemical impedance analyzer (Autolab PCSTAT 20 apparatus). Data collection, display and analysis is controlled by the FRA (v. 4.9) software.

2.2. Weight-loss measurements

Lead alloy rods with composition of those mentioned in the previous section were used for weight-losses measurements. After adding selenium in different concentrations to the alloy, the melt was poured in the cast iron mould and cast rods with surface area of 8cm² were removed from the moulds at about 140°C. The exact amount of selenium was measured with atomic absorption spectrometer (Analyst 100). Before each experiment, the rods were washed, degreased with acetone, rinsed with double-distilled water, dried, weighted and introduced in 1.28 sp.gr. H₂SO₄ solution. The rods were polarized with current density of 10 mAcm⁻² galvanostatically for 24h. Then, they were tacked out from the solution. All corrosion products were removed with hot alkaline saccharose solution. Then the rods rinsed with water, dried and weighted. Four rods were used for every alloy composition and a new test piece was used for each experiment.

2.3. Optical microscopy

Optical microscopy was used to study the microstructure of the alloys with different concentrations of selenium and its effect on the grain boundaries and sizes. For this purpose, the rods were mounted and polished mechanically with emery papers 800, 1500, 2500. All samples were degreased with acetone, washed with double-distilled water and etched. Finally, their etched surfaces were examined with optical microscopy apparatus (Zeiss- Neophot 32).

2.4. Discharge capacities

At first, the grids with identified compositions of selenium were casted by a 6SB₃ motorcycle's mould. Positive paste was prepared by mixing lead oxide supplied by Niru Battery Mfg CO., with water, sulfuric acid, according to conventional formulation in the manufacture of motorcycle MF batteries. The paste was then manually applied onto the grids with a plastic scraper. The pasted plates were cured at 60 °C with a relative humidity over 90% for 48 h in a curing set (VC 4018 m. ultra - Vit). The used cell for this test consists of one positive plate Pb-Sb-As alloy (with various concentrations of selenium) and two negative plates Pb-Ca alloys (that pasted, cured and charged previously) of a 6SB₃ motorcycle MF battery. The electrolyte was sulfuric acid with specific gravity of 1.28. The discharge capacity variations of the 2V cells were assessed by employing a solartron 1470, a multi- channel battery tester system. An initial formation algorithm was performed in 1.05 sp.gr. H₂SO₄ solution. This procedure consists of:

- 1- Rest for 0.5 h
- 2- Constant 10mA/g for 3.33 h
- 3- Constant 20mA/g for 5 h
- 4- Constant 30mA/g for 4.45 h
- 5- Rest for 0.5 h
- 6- Constant 33.33mA/g for 1 h
- 7- Rest for 0.5 h
- 8- Constant 6.66mA/g for 1 h
- 9- Rest for 10min

The formation was completed with repeating the steps for two times.

3. RESULTS AND DISCUSSION

3.1. Electrochemical studies

Potentiodynamic sweeping method is one of the most popular methods to study the reactions that proceed during corrosion reactions. Fig.1 shows the Tafel polarization curves of Pb-1.8wt% Sb - 0.1wt% As alloys with different concentrations of selenium. The region in Fig.1 is the active region in

which the electrodes corrode as the applied potential is made more positive and corresponds to $Pb \rightarrow PbSO_4$ reaction. Corrosion parameters are given in Table1. It can be seen from Fig.2 that with increasing selenium content, E_{corr} shifts to slightly negative potentials. Both anodic and cathodic slopes

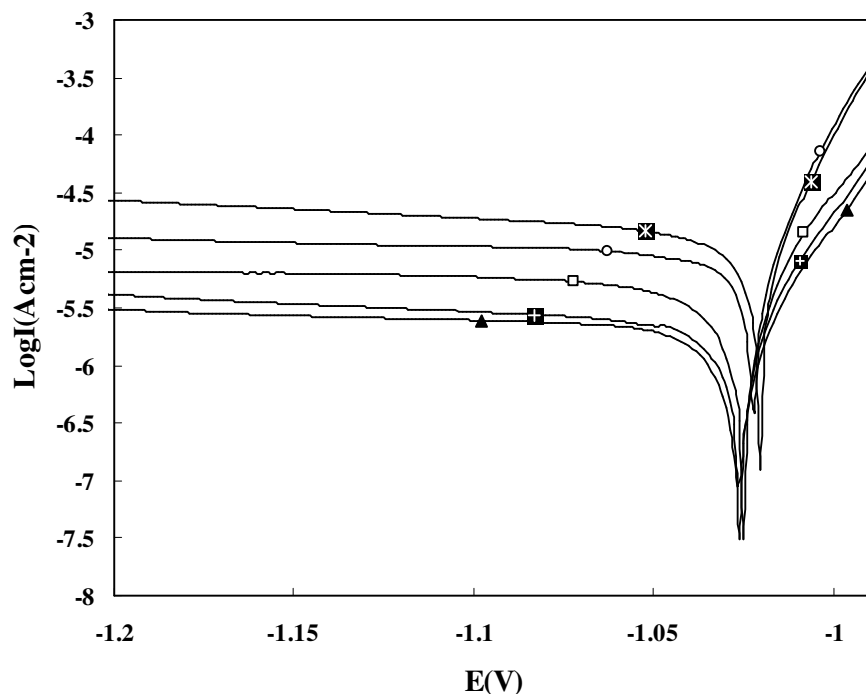


Figure 1. Polarization curves of the selenium effect on Pb-Sb-As alloys in 1.28 sp.gr. H_2SO_4 solution

Table 1. Corrosion data for Pb-Sb-As-Se alloys with different concentrations of selenium obtained from potentiodynamic sweeping method

Concentration (wt %)	$R_{ch}(\Omega cm^2)$	$C_{dl}(F cm^{-2})$	E (%)
Without	$3.3470 \cdot 10^{+2}$	$2.2049 \cdot 10^{-5}$	0
0.0070	$5.6091 \cdot 10^{+2}$	$1.1091 \cdot 10^{-5}$	40.32
0.0108	$8.6082 \cdot 10^{+2}$	$4.9131 \cdot 10^{-6}$	61.11
0.0141	$1.1909 \cdot 10^{+3}$	$2.6614 \cdot 10^{-6}$	71.89
0.0207	$1.7760 \cdot 10^{+3}$	$1.2396 \cdot 10^{-6}$	81.15

change and it indicates that selenium addition can affect both cathodic and anodic reactions that they are hydrogen evolution reaction and Pb oxidation respectively. Generally, with increasing selenium concentration, the corrosion current density and corrosion rate decrease and polarization resistance increases. It can be seen that with increasing selenium amount to 0.0108wt%, corrosion rate decreases 2.6 order of magnitude and with increasing its concentration to 0.0207wt% corrosion rate decreases

57.2 order of magnitude with respect to the base alloy without selenium. So, it shows that selenium effect on corrosion is more observable on high concentrations and high corrosion resistance alloys can be obtained with Se addition. Fig.3 shows the cyclic voltammograms of the alloys with different concentrations of selenium. The voltammograms were recorded in the PbO₂/PbSO₄ couple potential region (0.9-1.6 V) for 50 cycles and their 50th cycles were compared in Fig.3. The maximum peak current values, i_{pmax} , can be used to compare the stability of the anodic layer of different electrodes under a cycling condition, which is a close simulation of the condition when a battery works under cycling charge-discharge processes.

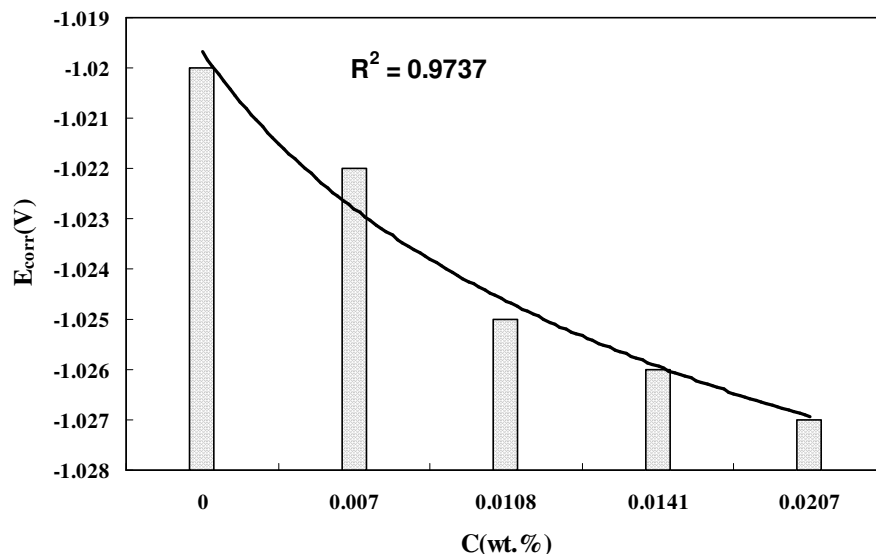


Figure 2. E_{corr}. vs. concentration variations for Pb-Sb-As-Se alloys in PS method

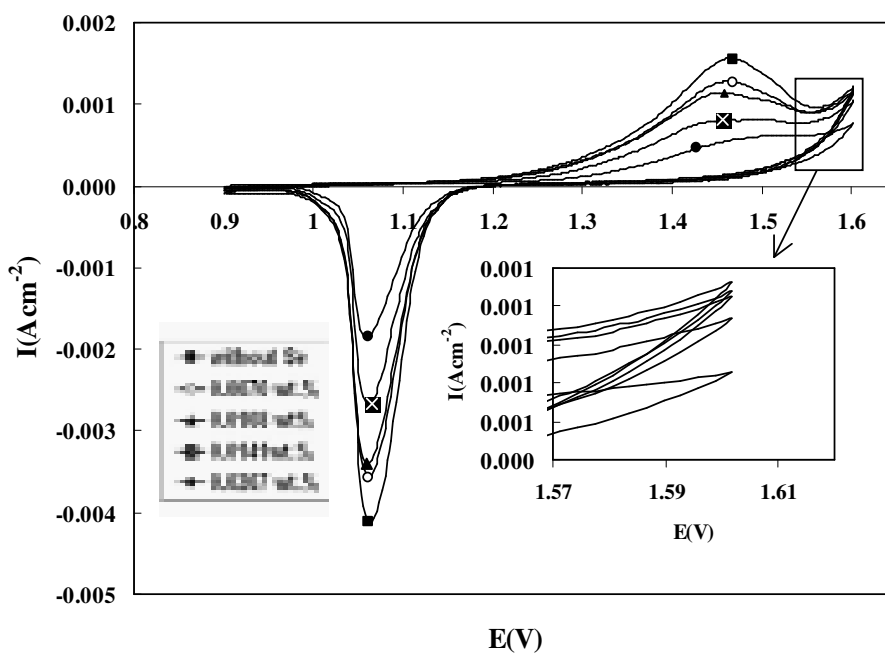


Figure 3. Cyclic voltammograms of Pb-Sb-As-Se electrodes between 0.9-1.6V in 1.28 H₂SO₄ solution; sweep rate=20mVs⁻¹

Also, Fig.3 provides information of the effect of Se addition on the $\text{PbSO}_4 \leftrightarrow \text{PbO}_2$ reactions. The results suggest that the Se additions vary the kinetic barrier for the formation of PbO_2 from PbSO_4 and inhibit the oxidation of PbSO_4 to PbO_2 .

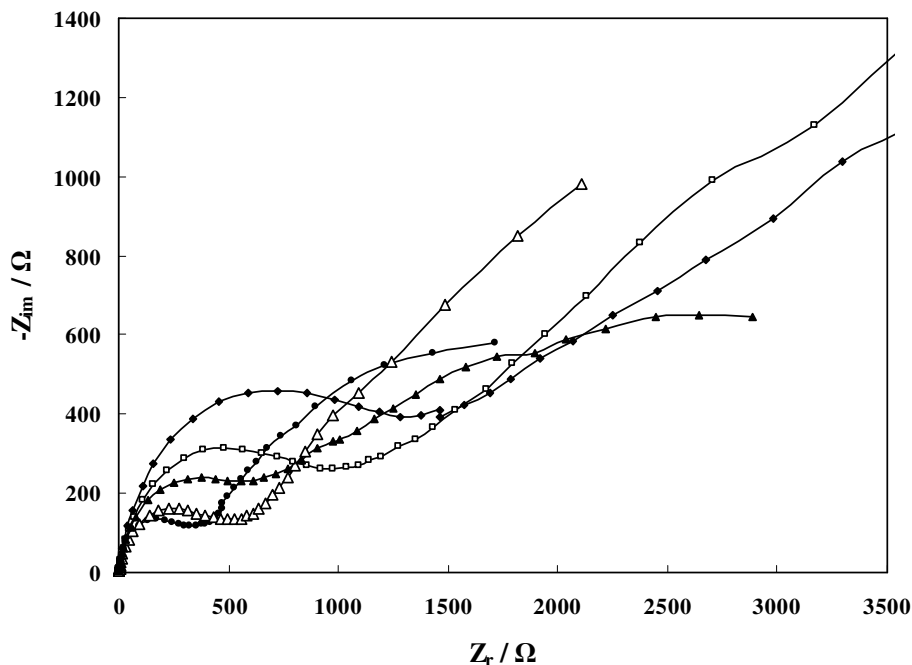


Figure 4. Nyquist plots of Pb-Sb-As-Se alloy electrodes with different selenium content at 1.45V

Electrochemical impedance spectroscopy has been already applied in studies of lead-acid battery system. For example, Hampson and Kelly have measured the impedance of PbO_2 films formed on pure lead and lead-calcium alloys [16]; recently Brinic et al.[17] reported the results from EIS measurements on lead and lead-antimony alloys in lead sulphate and lead dioxide potential regions.

Impedance measurements were carried out in a frequency of 100 kHz to 1mHz with amplitude of 10 mV peak-to-peak using ac signals. Electrochemical impedance measurements were performed by using the lead alloys as working electrodes coated with thin layer of $\beta\text{-PbO}_2$. For this test, the working electrode was controlled at a constant potential of 1.45V for 40min, to produce a stable film of $\beta\text{-PbO}_2$ and then impedance measurements were performed in the range of 100 kHz to 1 mHz. Fig.4 shows the Nyquist plots of impedance of electrodes. The charge transfer resistance values (R_{ct}) are calculated from the difference in impedance at lower and higher frequencies on capacitive loop, as described Elsevier [18]. To obtain the double layer capacitance (C_{dl}) the frequency at which the imaginary part of the impedance is maximum $(-Z_{im})_{max}$ is found and C_{dl} values are calculated from the following equation[19]:

$$C_{dl} = \frac{1}{W_{max} R_{ct}}$$

The interpretation of Nyquist Fig.4 allows to determine the electrochemical parameters of lead alloy electrodes and to acquire information about the corrosion process and mechanism. As in table2, the corrosion rate can be calculated by determining the reciprocal of charge transfer resistance ($\frac{1}{R_{ct}}$).

Data in table2 shows the selenium obviously inhibits the corrosion of lead alloys in 1.28 sp.gr. H₂SO₄ solution. The inhibition efficiency increased by increasing the concentration of selenium. The inhibition efficiency is calculated using charge transfer resistance from equation [19]:

$$E\% = \frac{R_{ct}^{add} - R_{ct}}{R_{ct}^{add}} \times 100$$

Where R_{ct} and R_{ct}^{add} are the charge transfer resistance values in absence and presence of selenium (as an alloying additive for the lead alloys), respectively. By increasing selenium concentration, the R_{ct} values increased but C_{dl} values decrease. The Nyquist plots of Fig.4 show that the polarization resistance increases, which indicates that the dissolution rate of the β -PbO₂ film on the alloys decreases and the film becomes more stable when the Se content increases. This result is in agreement with anodic polarization and cyclic voltammetric measurements.

Table 2. Impedance data of Pb-Sb-As alloys with different concentrations of selenium

Concentration (wt %)	$R_{ch}(\Omega\text{cm}^2)$	$C_{dl}(\text{F cm}^{-2})$	E (%)
Without	3.3470×10^2	2.2049×10^{-5}	0
0.0070	5.6091×10^2	1.1091×10^{-5}	40.32
0.0108	8.6082×10^2	4.9131×10^{-6}	61.11
0.0141	1.1909×10^3	2.6614×10^{-6}	71.89
0.0207	1.7760×10^3	1.2396×10^{-6}	81.15

3.2. Hardness

Fig.5 illustrates that selenium addition increases hardness of the alloys. The curve shows the as-cast grids hardness versus selenium content of the alloys after one week (under atmospheric condition). Selenium in the alloys compositions acts as a stabilizer for the antimony and grain refiner. The selenium addition was intended to reduce or eliminate the tendency of the grids to crack upon cooling after casting. Also, selenium increases homogeneity of the alloy structure, it removes columnar structures and makes the alloy corrosion resistant.

3.3. Weight-loss measurements

Weight-losses of Pb-Sb-As alloy rods with different concentrations of selenium as an alloying additive (with 8cm² surface area) in 1.28sp.gr. H₂SO₄ solutions were measured after 24h

galvanostatically polarization with current density of 10mAcm^{-2} . The used electrochemical cell has shown in Fig.6. Fig.7 shows the weight-losses and inhibition efficiencies against selenium concentrations in the alloys. It can be seen that with increasing selenium amount, weight-losses decrease and the inhibition efficiencies increase reciprocally and weight-loss of lead alloy depends on concentration of selenium.

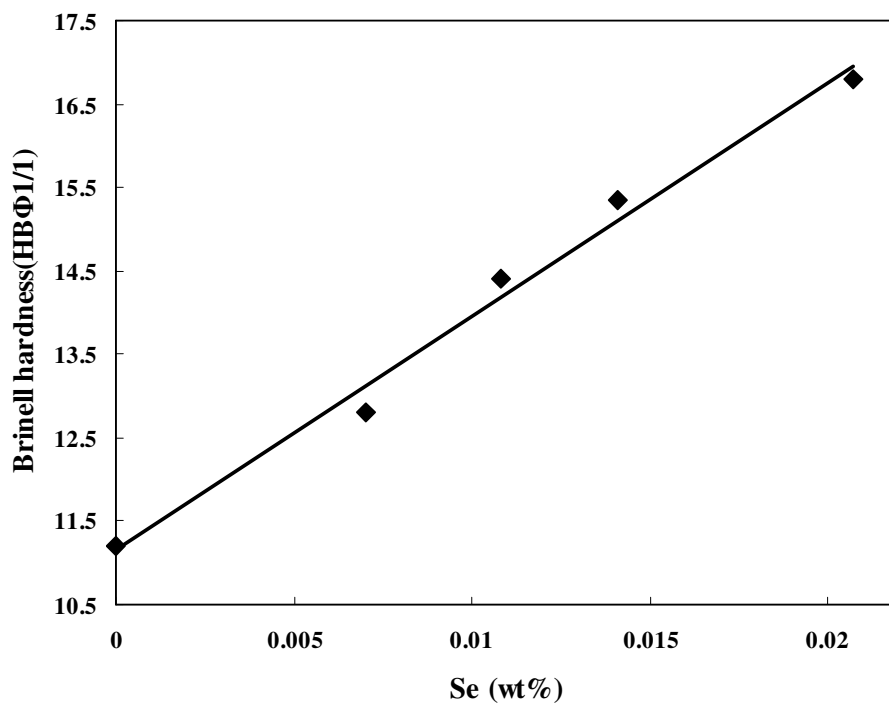


Figure 5. Hardness of Pb-Sb-As-Se alloys after one week

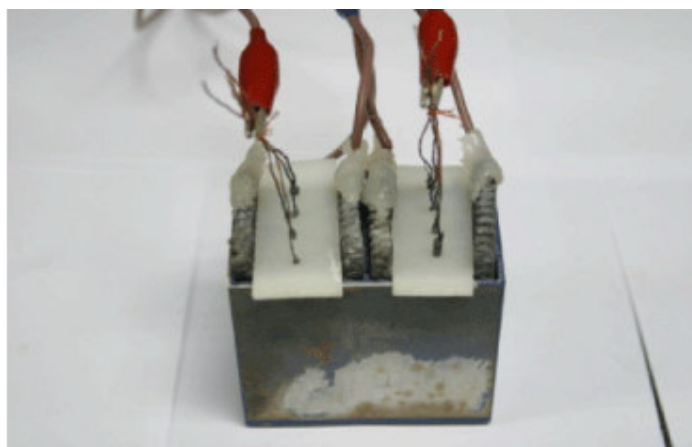


Figure 6. Electrochemical cell used for weight losses measurements

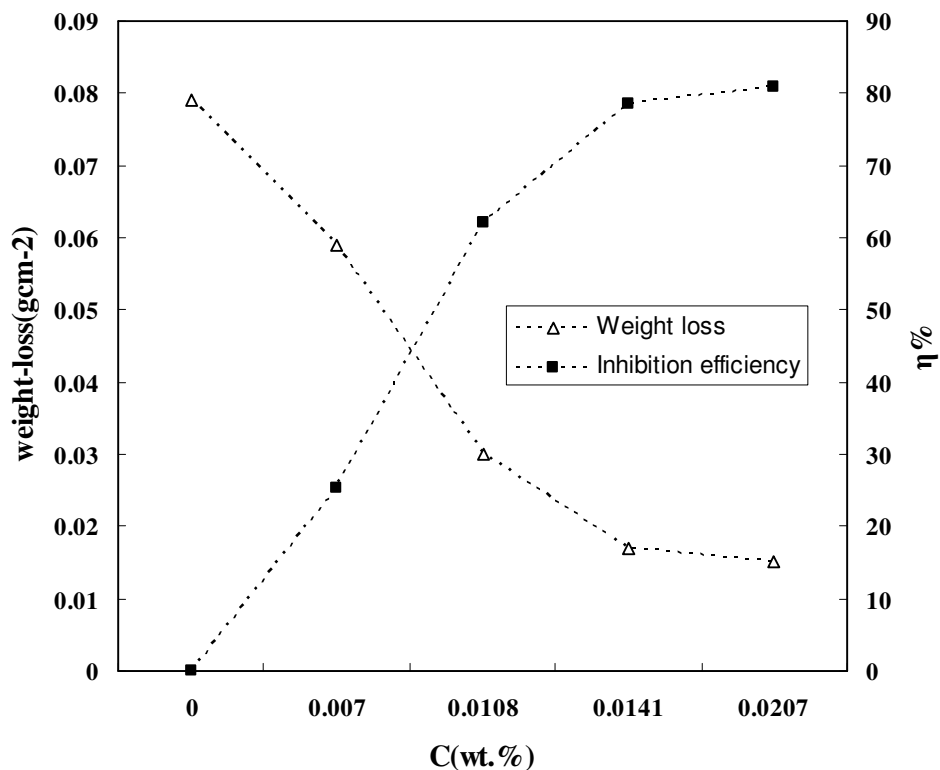


Figure 7. weight-losses and inhibition efficiencies against selenium concentration curves for Pb-Sb-As-Se alloys

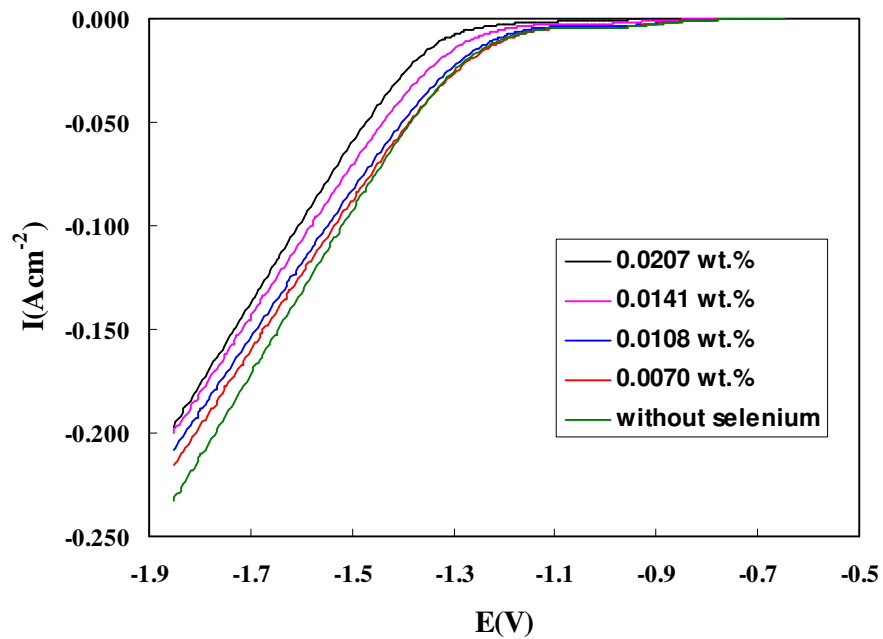


Figure 8. Hydrogen evolution reaction rate at 50th cycle on Pb-Sb-As-Se alloy electrodes with different selenium addition; sweep rate= 20mVs⁻¹ in 1.28 H₂SO₄ solution T=25°C

3.4. Gas evolution measurements

Hydrogen evolution reaction rate of the alloys with different concentrations of selenium was measured with cyclic voltammetry method by scanning the potential in hydrogen evolution potential region. Fig.8 shows the voltammograms of the hydrogen evolution reaction rate. The results show that, with addition of selenium, the overpotential of hydrogen evolution reaction increases. With battery cycling, antimony migrates to the negative electrodes and increases hydrogen evolution. Selenium leads to uniform distribution of antimony and suppresses hydrogen evolution.

The oxygen evolution reaction occurs at the anodic layer- electrolyte interface and its rate is affected by quantity of PbO_2 on the electrode. The electrodes of alloys with different concentrations of selenium were cycled in the oxygen evolution potential region. Tests were performed after the working electrodes were hold at a constant potential of 1.45V for 60min to produce a steady film of PbO_2 and then were swept with 20mVs^{-1} from 1.2V to 1.5V. The results of 50th cycles are shown in Fig.9 and it shows that addition of selenium increases oxygen evolution overpotential and decreases its rate. Probably selenium decreases the number of active centers available for the oxygen evolution.

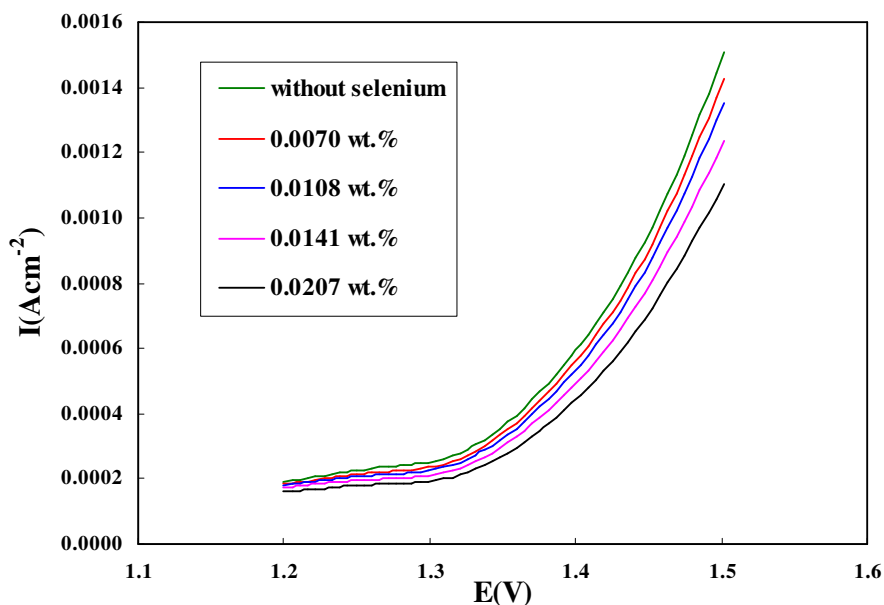


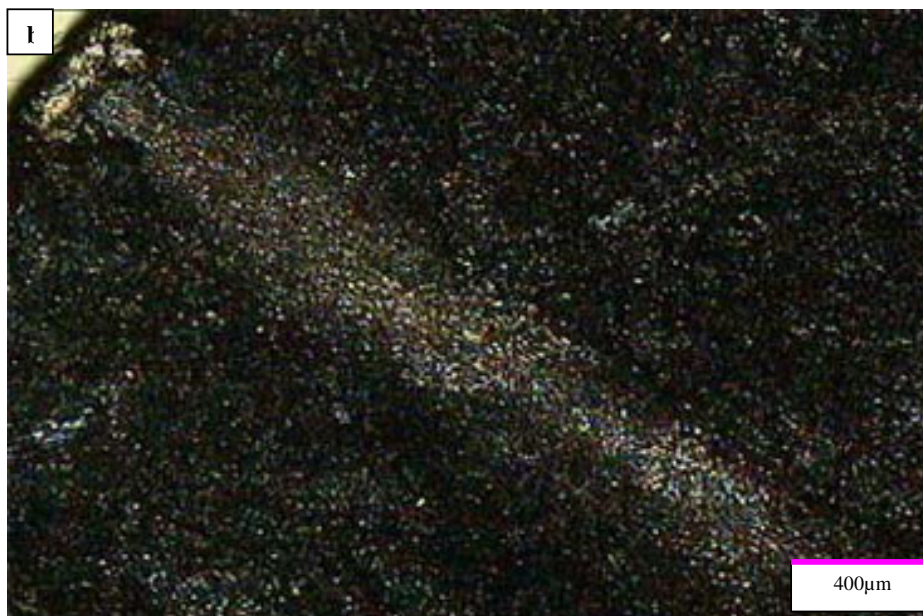
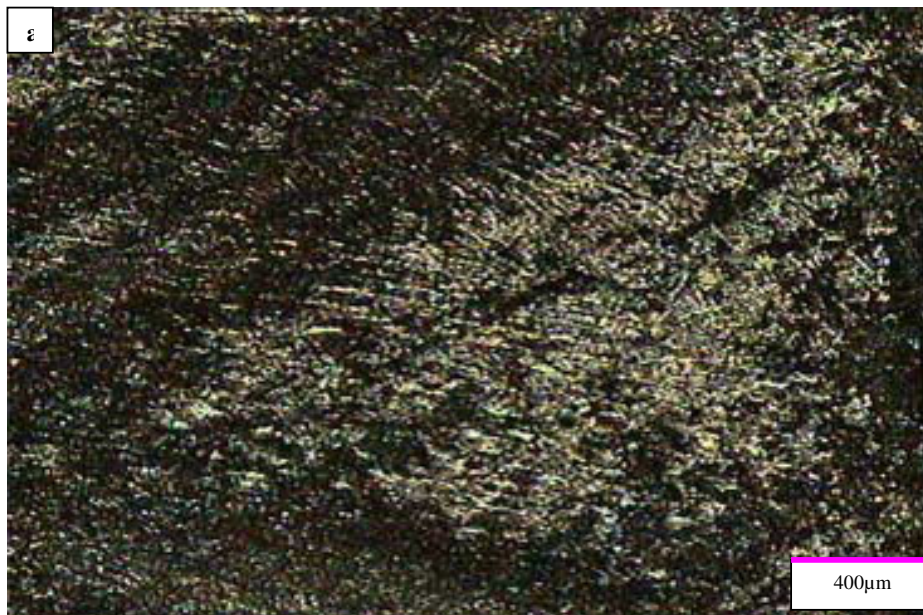
Figure 9. Oxygen evolution reaction rate at 50th cycle on Pb-Sb-As-Se alloy electrodes with different selenium additions; sweep rate= 20mVs^{-1} in $1.28\text{H}_2\text{SO}_4$ solution, $T=25^\circ\text{C}$

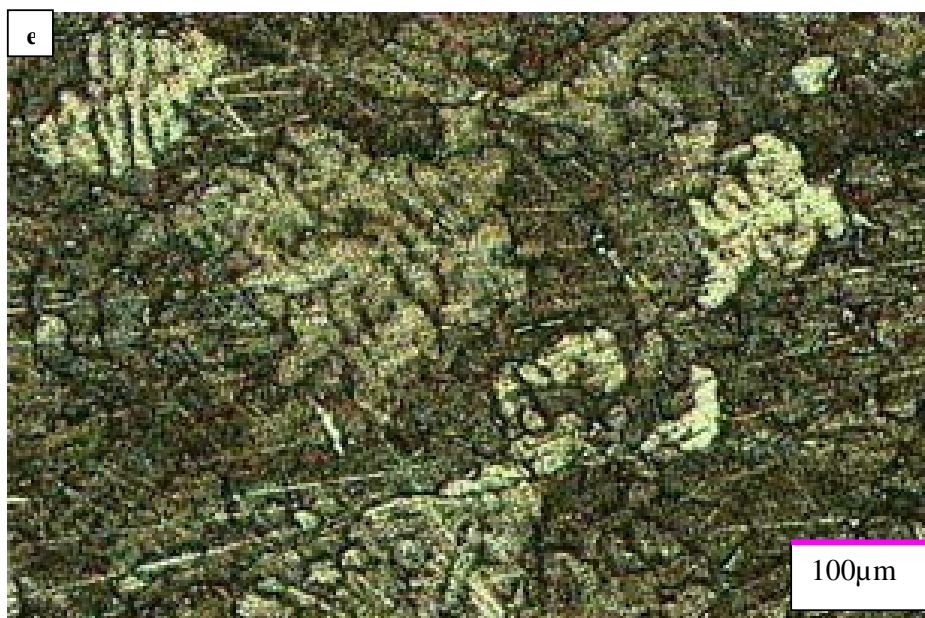
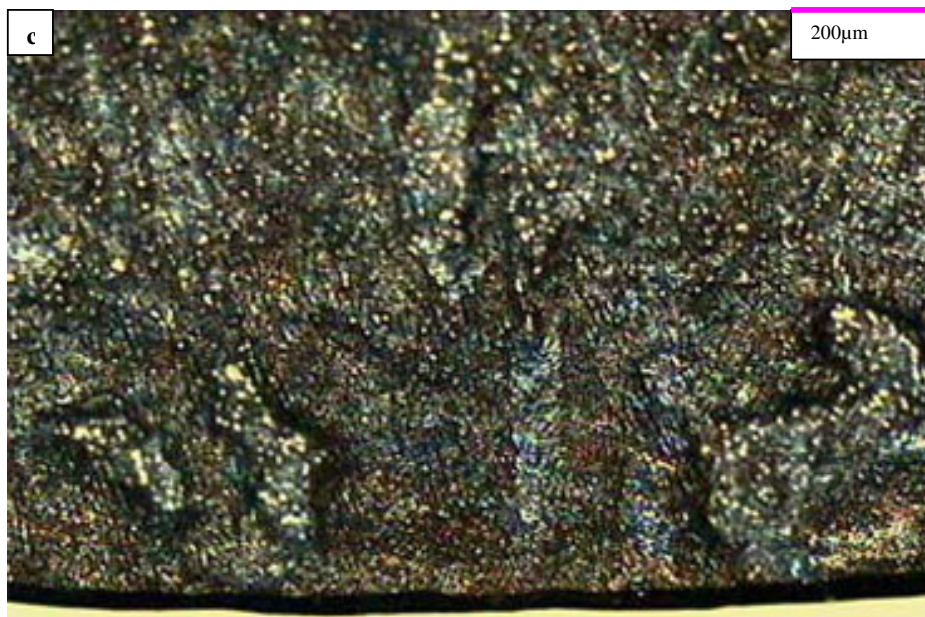
3.5. Optical microscopy

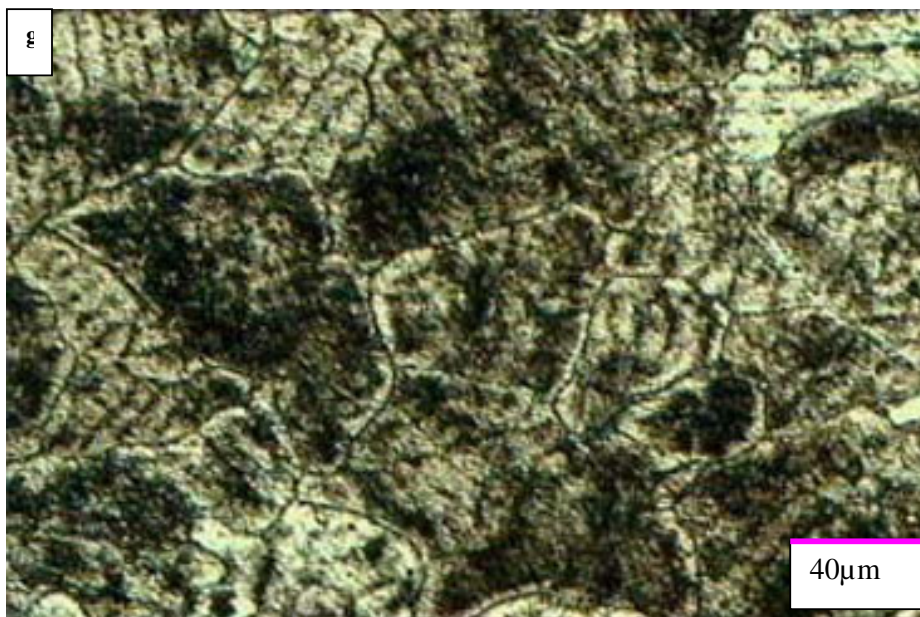
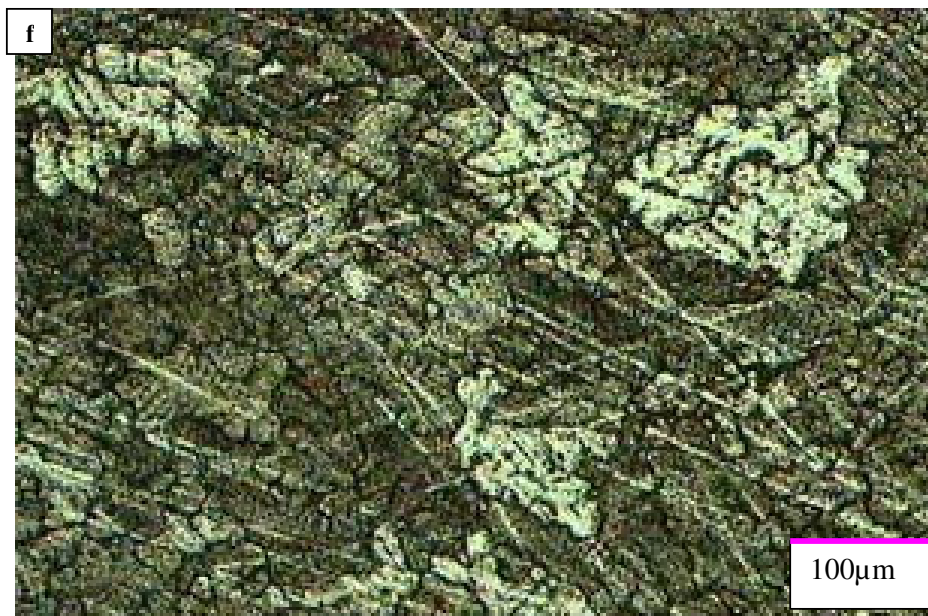
The microstructures of Pb-Sb-As alloys with different concentrations of selenium were investigated to determine the effect of this additive on the grain size and grain boundaries of the alloys. Fig.10 shows the cast structure of grids containing different concentrations of selenium. It can be seen that with increasing selenium concentrations grain size reduces and its shape changes from columnar to round and globulitic form. The solidification takes place in a coarse dendritic structure containing cracks along grain boundaries. Insufficient grid quality (caused by these cracks) was one of the main

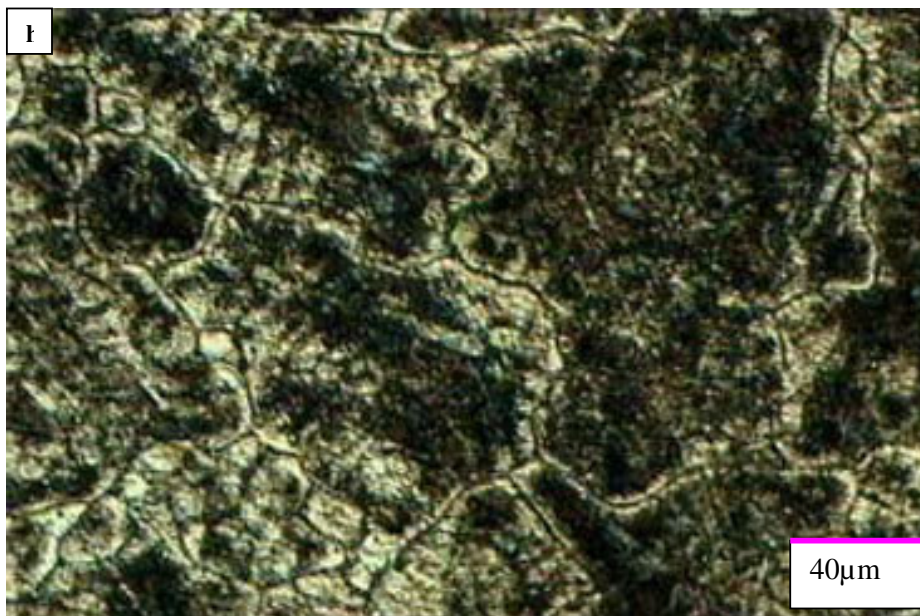
reasons why lead-antimony alloys were formerly not used on a large scale in the industry. Selenium addition forms a fine globulitic solidification which is free from casting faults. The formation of dendrites which disturbs the feeding capacity of the mould during casting and leads to casting faults is almost fully suppressed. With fine globulitic solidification uniform mechanical properties are achieved in all directions and hence the ductility is increased.

The combination of alloying elements (antimony, selenium, arsenic) with lead makes it possible to manufacture battery grids with low antimony alloys which achieves the necessary mechanical strength within suitable ageing times and shows the necessary grid quality.









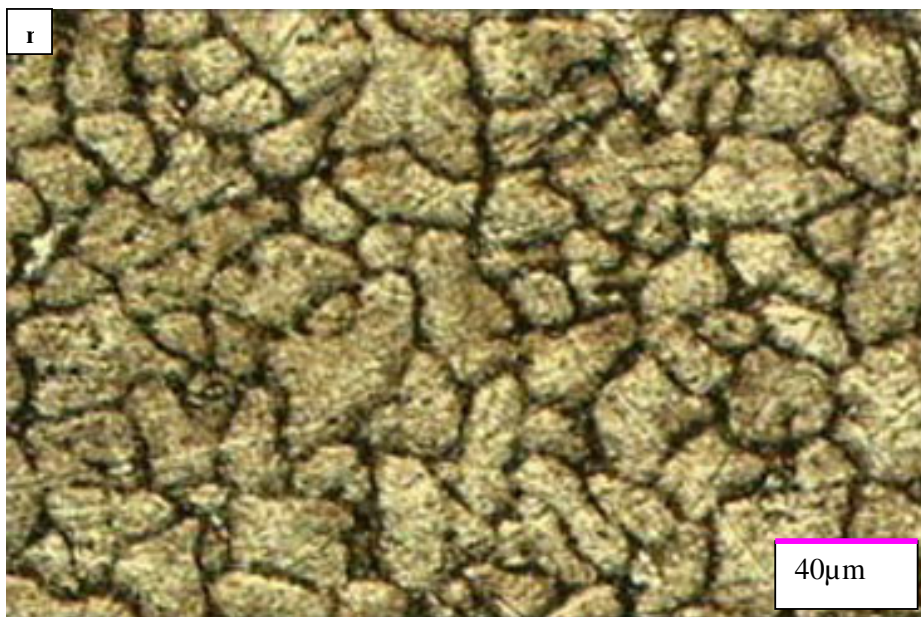


Figure 10. Optical microscopy images of etched Pb-Sb-As-Se samples with different selenium concentrations, key: (a,b) without selenium, (c) 0.0070 wt.%, (e,f) 0.0108 wt.%, (g,h) 0.0141 wt.%, (k,m) 0.0207 wt.%

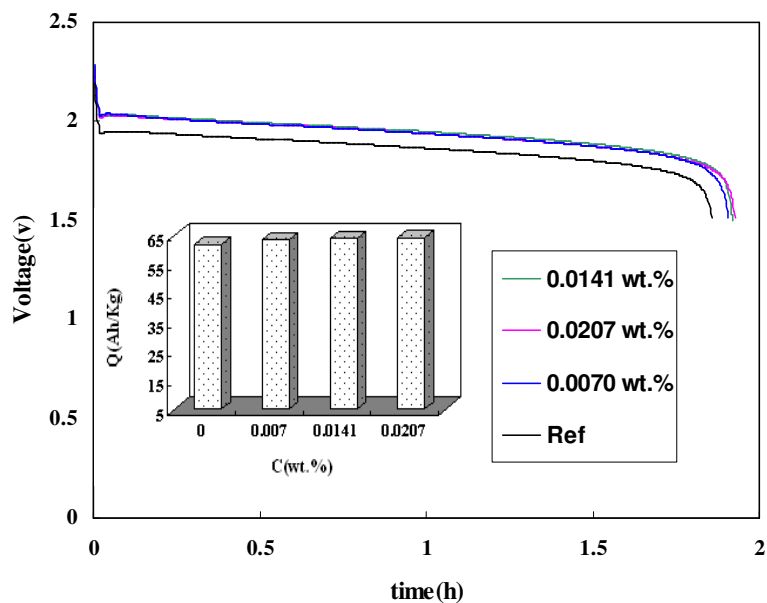


Figure 11. Voltage/ time curves for different percentage of selenium as an additive during 5th discharge process by constant current of 1 A

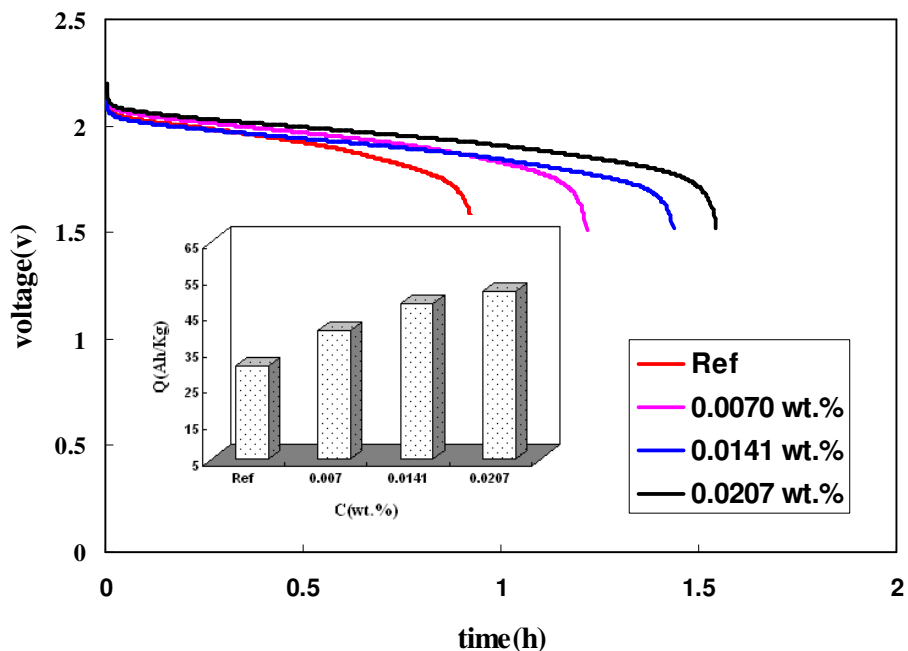


Figure 12. Voltage/ time curves for different percentage of selenium as an additive during 15th discharge process by constant current of 1 A

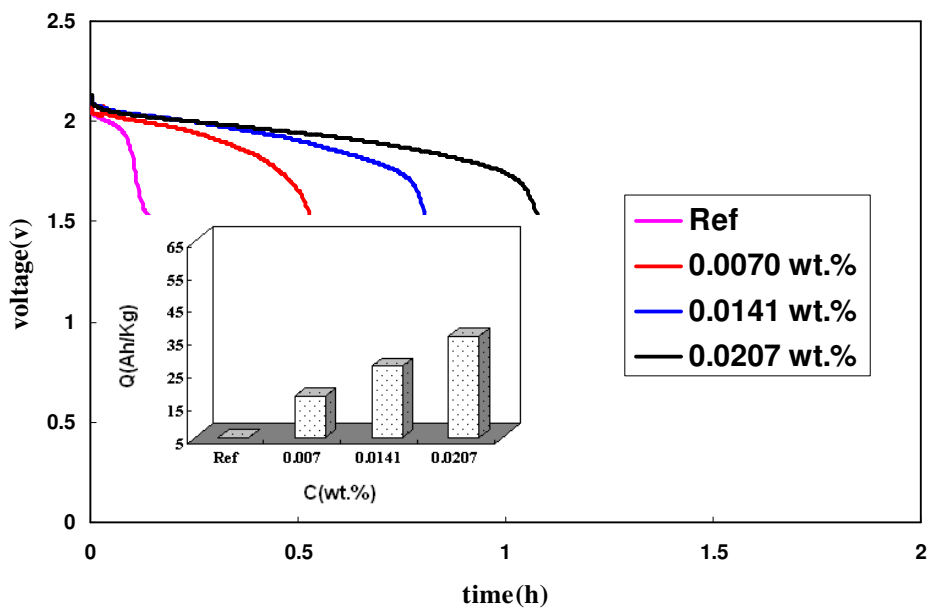


Figure 13. Voltage/ time curves for different percentage of selenium as an additive during 25th discharge process by constant current of 1 A

3.6. Discharge capacities

The cells were discharged at -1A until the voltage had fallen to 1.5V and charged at 0.9A until the voltage had risen to 2.6V. The electrolyte was 1.28 sp.gr. H₂SO₄ solution and the charge/discharge procedure was repeated for 25 cycles. The time-voltage behaviors of cells with different contents of selenium during discharge process were shown at Fig.11 for 5th cycles. The discharge capacities for these cells were calculated and shown in the related figure. The capacity tests for Se-doped grids were slightly higher than of Se-free grids (Fig.11). Nevertheless, this difference was not meaningful during primary cycles. Fig.12 and Fig.13 show the discharge behavior of the alloys for 15th and 25th cycles respectively. As cycling proceeds, the beneficial effect of selenium on the discharge capacities becomes more and more. As it could be seen from these figures, the discharge time for the cells containing 0.0207wt.% of selenium is the highest. In this concentration, discharge capacity has a notable increase for 15th and 25th cycles with respect to the cells without selenium and the addition of selenium has beneficial effect on discharge capacities of hybrid lead-acid batteries during the later cycles. This can probably be related to a good corrosion resistance of the alloys involving of selenium. Because, the exceedingly corrosion layer thickness, causes a decrease in the adhesion of the paste on the grids and finally the paste starts shedding.

4. CONCLUSIONS

Influence of selenium on the electrochemical behavior, corrosion resistance, gas evolution and microstructure of Pb-Sb-As base alloy was investigated. The results of potentiodynamic sweeping method show that with increasing selenium content, E_{corr} shifts to slightly negative potentials. Both anodic and cathodic slopes change and it indicates that selenium addition can affect both cathodic and anodic reactions. The corrosion current density and corrosion rate decrease and polarization resistance increases. Cyclic voltammetry technique shows that selenium effect on the corrosion of the alloy is more observable on high concentrations and it varies the kinetic barrier for the formation of PbO₂ from PbSO₄ and inhibits the oxidation of PbSO₄ to PbO₂. Also, addition of selenium increases the overpotential of both hydrogen and oxygen evolution reaction and decreases their evolution reaction rate. The Nyquist plots show that with increasing selenium concentration the dissolution rate of the β -PbO₂ film on the alloys decreases and the film becomes more stable. Optical microscopy method shows that addition of selenium reduces the grain size and changes their shapes from columnar to round and globulitic forms. Hardness of the alloys with increasing selenium concentration increases. The addition of selenium in the positive grids of hybrid lead-acid batteries is beneficial for discharge capacities of positive electrodes during the later cycles.

ACKNOWLEDGEMENTS

The authors would like to acknowledge Niru Battery Manufacturing Company specially Mr. S.M. Tabaatabaai for supporting this study.

References

1. N.E. Bagshaw, *J. power Sources*, 53 (1995) 25
2. D. Berndt, S. C. Nijhawan, *J. Power Sources*, 1 (1976/77) 3
3. C. O. Donnel, C. Finin, *Mesa Technical Associates, Inc.*,
4. A. Nuzhny, *J. Power Sources*, 158 (2006) 920
5. Hebbar; Ranna K. ; Rao; M. Vikram; Foerster; George S., US Patent, 4,158,563 (1979)
6. C. Ronglong, W. Shousong, *J. Power Sources*, 46 (1993) 327
7. P. Rao, S. R. Larsen, Us Patent, 5,650,242, (1997)
8. P. Rakin, *J. Power Sources*, 36 (1991) 461
9. D. Pavlov, M. Dimitrov, G. Petkova, *J. Electrochem. Soc.*, 142 (1995) 2919
10. R. K. Hebbar, M. V. Rao, G. S. Foerster, US Patent, 4,158,563, (1979)
11. N. E. Bagshaw, *J. Power Sources*, 33 (1991) 3
12. K. Peters, US Patent, 3,912,537 (1975)
13. S. Nijhawan, US Patent, 3,801,310 (1974)
14. S. C. Nijhawan, W. Berger, US Patent, 3,990,893 (1976)
15. A. Ueberschaer, U. Heubner, M. Reinert, US Patent, 3,993,480 (1976)
16. N. A. Hampson, S. Kelly, *J. Appl. Electrochem.* 11(1981) 751
17. S. Brinic, M. Meticos-Hukovic, R. Babic, *J. Electrochem. Soc.*, 55 (1995) 19
18. S. S. Abdel-Rahim, Magdy A. M. Ibrahim, K. F. Khaled, *J. Appl. Electrochem.* 29 (1999) 593
19. K. F. Khaled, *Appl. Surf. Sci.*, 230(2004) 307